Vapor Condensation on Liquid Surface Due to Laminar Jet-Induced Mixing

C. S. Lin*
Analex Corporation, NASA Lewis Research Center, Cleveland, Ohio 44135
and
M. M. Hasan*
NASA Lewis Research Center, Cleveland, Ohio 44135

The effects of system parameters on the interface condensation rate in a laminar jet-induced mixing tank are numerically studied. The physical system consists of a partially filled cylindrical tank with a subcooled jet discharge from the center of the tank bottom toward the liquid-vapor interface which is at a saturation temperature corresponding to the constant tank pressure. Liquid is also withdrawn from the outer part of the tank bottom to maintain the constant liquid level. The steady-state conservation equations in nondimensional form are solved by a finite-difference method for various system parameters including liquid height to tank diameter ratio (H/D), tank to jet diameter ratio (D/d), liquid outflow to jet area ratio (A_{out}/A_j), and a heat leak parameter (Nh) which characterizes the uniform wall heat-flux. It is found that the average condensation Stanton number ($\overline{St}_c$) is decreasing with increasing H/D, D/d, and Nh. For small Nh, $\overline{St}_c$ is nearly independent of A_{out}/A_j. For $Re_j \leq 600$, $\overline{St}_c$ is essentially equal to $(d/D)^2$ if $(D/d) \geq 20$ and $Nh \ll 1$.

Nomenclature

A = surface area of central jet, outflow, or interface
B = tank to jet diameter ratio, D/d
C_p = specific heat at constant pressure for liquid region
$C_{p,v}$ = specific heat at constant pressure for vapor region
D = tank diameter
d = jet diameter
g = gravitational acceleration
H = liquid height from the tank bottom
h_c = condensaton heat-transfer coefficient
h_{fg} = latent heat of condensation
Ja = Jakob number, $C_p(T_s - T_j)/h_{fg}$
k = thermal conductivity
m_c = condensation mass flux
Nh = wall heat-flux parameter, $(q_w D)/[k(T_s - T_j)]$
p = pressure
p_g = equilibrium hydrostatic pressure, $\partial p_g/\partial x = -\rho g$
p^* = dimensionless pressure, $(p - p_g)/\rho u_j^2$
Q = jet volume flow rate
q_w = tank wall heat flux
Re_j = jet Reynolds number, $\rho u_j d/\mu$
r = radial coordinate measured from the centerline
r^* = dimensionless radial coordinate, r/D
St_c = condensation Stanton number, $h_c/\rho u_j C_p$
T = temperature
T^* = dimensionless temperature, $(T - T_j)/(T_s - T_j)$
u = axial velocity
u_c = condensation-induced velocity (positive value)
u^* = dimensionless axial velocity, u/u_j
u_c^* = dimensionless condensation-induced velocity, u_c/u_j
v = radial velocity
v^* = dimensionless radial velocity, v/u_j
v_s^* = dimensionless radial velocity at interface
x = axial coordinate measured from the tank bottom
x^* = dimensionless axial coordinate, x/D
x_p = potential core length
μ = dynamic viscosity
ρ = liquid density
— = average value over the interface

Subscripts
c = evaluated at condensation condition
j = evaluated at jet inlet
out = evaluated at outflow location
s = evaluated at liquid-vapor interface
v = evaluated at vapor condition

Presented as Paper 90-0354 at the AIAA 28th Aerospace Sciences Meeting, Reno, NV, Jan. 8–11, 1990; received Feb. 13, 1990, revision received Sept. 14, 1990; accepted for publication Sept. 21, 1990.

*Research Engineer, Cryogenic Fluids Technology Office. Member AIAA.

Introduction

THE pressure control of cryogenic storage tanks in space is one of the major technologies being developed in the NASA cryogenic fluids management program. The heat transferred through insulated tank walls can result in thermal stratification of the cryogenic propellant which increases the tank self-pressurization rate. A preferred method of controlling the pressure of a cryogenic storage system is the use of axial jet-induced mixing.[1,2] A slightly subcooled jet can provide mixing of tank liquid and transfers heat from the interface into the bulk liquid. Vapor condensation is induced and the pressure of the tank is then reduced. Therefore, the interface condensation plays the key role in controlling the pressure of a jet-induced mixing tank.

Several studies of steady-state fluid mixing and condensation rate have been conducted. Thomas[3] measured the condensation rate of steam on water surfaces mixed by a submerged turbulent jet and found that the condensation rate was roughly proportional to the jet Reynolds number. Dominick[4] investigated the effects of jet injection angle and jet flow rate on the condensation rate in a Freon 113 tank. The interface heat transfer was observed to increase as jet injection angle became more normal to the interface. However, the average heat transfer coefficient at the interface was found to be increasing with jet Reynolds number only to a power of 0.73. Sonin et al.[5] measured the steady-state condensation rate of steam in a water tank with condensation

process dominated by the liquid-side turbulence near the interface. A correlation between the condensation rate and characteristic interface turbulent velocity was developed. Hasan and Lin[6] used a finite-difference method to solve time-averaged conservation equations along with a k-ε turbulence model for the prediction of turbulent velocity. The numerical prediction was in good agreement with Sonin's data except for the region close to the interface where the diffusion process was dominant. The effects of flow parameters, such as jet Reynolds number and Prandtl number, on the interface condensation rate in a laminar jet-induced mixing tank were studied numerically by Lin.[7] The numerical results showed that the average condensation heat-transfer coefficient increased linearly with the jet Reynolds number and varied with the liquid Prandtl number to a power of about 0.97 for $0.85 \leq Pr \leq 2.65$.

Besides the flow parameters, the vapor condensation rate in a mixing tank is also dependent on the system parameters which affect directly the design of the mixing device. Lacking an adequate design data base, any overdesign of the mixing device will increase its weight and power consumption. This will lower the performance efficiency of the mixing device in reducing tank pressure. Presented in this paper are results of a numerical investigation on the effects of system parameters on the interface condensation rate and useful information for the design of a mixing device.

It has been shown[7] that for a small jet to tank diameter ratio most of the vapor condensation occurs in the central part of the interface so that the normal-gravity solution (flat interface) may be a good approximation to low-gravity condition (curved interface). Thus, flat interface assumption is used and only laminar flow is considered in the present investigation. However, it is expected that the effects of system parameters on the interface condensation process will be qualitatively the same for both the laminar and the turbulent jets.

Problem Formulation and Description

The physical system and the coordinates used to analyze the problem are shown in Fig. 1. A laminar axial-jet of diameter d is located at the center of the bottom of a cylindrical tank of diameter D. Liquid is continuously withdrawn from the outer portion of the tank bottom to maintain a constant liquid fill level. Both the central jet and outflow velocities, u_j and u_{out}, respectively, are assumed uniform. The effect of vapor superheat is neglected which implies that $C_{p,v}(T_v - T_s)/h_{fg} \ll 1$. Also, the effect of vapor motion on the condensation process is assumed to be negligible. The above assumptions effectively decouple the liquid region from the vapor region. Therefore, the condensation rate can be determined from the solution of the temperature field only in the liquid region.

The liquid-vapor interface is assumed to be flat (wave free), shear-free, and at a constant saturation temperature, T_s. The axial jet is at a constant subcooled temperature, T_j, and the tank outflow region is assumed to have zero temperature gradient. Tank walls are subjected to a uniform wall heat flux which is characterized by a dimensionless wall heat-flux parameter, $Nh(Nh \equiv (q_w D)/[k(T_s - T_j)])$. All the associated thermodynamics and transport properties are assumed constant since only small temperature variation is considered in the whole flowfield.

The energy and mass balance in the liquid region can be expressed, respectively, as

$$\int \rho u_{out} C_p T_{out} dA_{out} - \int \rho u_j C_p T_j dA_j = \int m_c h_{fg} dA_s + \int \rho u_c C_p T_s dA_s + \pi D H q_w \tag{1}$$

$$\rho u_{out} A_{out} - \int m_c dA_s = \rho u_j A_j \tag{2}$$

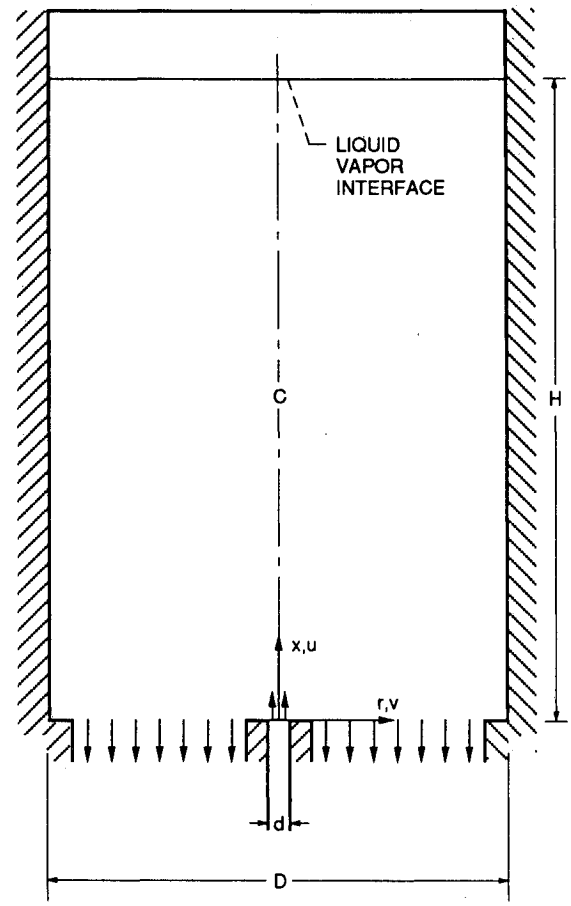

Fig. 1 Physical system and coordinates.

where m_c, h_{fg}, C_p, T_{out}, and q_w are the local interfacial condensation mass flux, latent heat of condensation, specific heat at constant pressure, local outflow temperature, and wall heat flux, respectively. The condensation-induced velocity is obtained by

$$u_c = \frac{m_c}{\rho} \tag{3}$$

By using Eqs. (2) and (3), Eq. (1) becomes

$$\int m_c dA_s = \frac{\rho Q\, Ja \left(\dfrac{\bar{T}_{out} - T_j}{T_s - T_j}\right) - \pi D H \dfrac{q_w}{h_{fg}}}{1 + Ja\left(1 - \dfrac{\bar{T}_{out} - T_j}{T_s - T_j}\right)} \tag{4}$$

where the jet volume flow rate (Q), the Jakob number (Ja), and the average outflow temperature are defined as $Q = u_j A_j$, $Ja = C_p(T_s - T_j)/h_{fg}$, and $\bar{T}_{out} = \int T_{out} dA_{out}/A_{out}$, respectively. The form of Eq. (4) is convenient to estimate the interfacial condensation mass flux by using the measurable experimental variables. The condensation mass flux at the interface is given by

$$\bar{m}_c h_{fg} A_s = \int m_c h_{fg} dA_s = \int \left(k \frac{\partial T}{\partial x}\right)_s dA_s \tag{5}$$

where $\bar{m}_c$ is the average condensation mass flux at the interface, and k is the thermal conductivity. Thus, the conden-

sation-induced velocity can be related to the interfacial temperature gradient by

$$u_c = \frac{k\left(\frac{\partial T}{\partial x}\right)_s}{\rho h_{fg}} \tag{6}$$

Equations (4) and (5) can be used as the termination criterion for the iterative calculation or as a check of the numerical solutions.

Mathematical Modeling

The jet-induced mixing problem considered in the present study is steady-state and incompressible with gravity acting in the vertical negative-x direction. The dimensionless forms of the governing equations, with buoyancy force resulting from the temperature gradient in the liquid neglected, are

$$\frac{\partial u^*}{\partial x^*} + \frac{\partial}{r^* \partial r^*}(r^* v^*) = 0 \tag{7}$$

$$\frac{\partial}{\partial x^*}(u^{*2}) + \frac{\partial}{r^* \partial r^*}(u^* r^* v^*) = -\frac{\partial p^*}{\partial x^*} + \frac{1}{B\,Re_j}\left[\frac{\partial^2 u^*}{\partial x^{*2}} + \frac{\partial}{r^* \partial r^*}\left(r^* \frac{\partial u^*}{\partial r^*}\right)\right] \tag{8}$$

$$\frac{\partial}{\partial x^*}(u^* v^*) + \frac{\partial}{r^* \partial r^*}(r^* v^{*2}) = -\frac{\partial p^*}{\partial r^*} - \frac{1}{B\,Re_j}\frac{v^*}{r^{*2}} + \frac{1}{B\,Re_j}\left[\frac{\partial^2 v^*}{\partial x^{*2}} + \frac{\partial}{r^* \partial r^*}\left(r^* \frac{\partial v^*}{\partial r^*}\right)\right] \tag{9}$$

$$\frac{\partial}{\partial x^*}(u^* T^*) + \frac{\partial}{r^* \partial r^*}(r^* v^* T^*) = \frac{1}{B\,Re_j\,Pr}\left[\frac{\partial^2 T^*}{\partial x^{*2}} + \frac{\partial}{r^* \partial r^*}\left(r^* \frac{\partial T^*}{\partial r^*}\right)\right] \tag{10}$$

Boundary conditions are required to solve the elliptic Eqs. (7) to (10). At the centerline, the symmetric conditions are used

$$v^* = 0, \frac{\partial u^*}{\partial r^*} = \frac{\partial T^*}{\partial r^*} = 0$$

Nonslip conditions are applied to the solid walls

$$u^* = v^* = 0$$

The bottom-wall is assumed to be adiabatic

$$\frac{\partial T^*}{\partial x^*} = 0$$

The side-wall is subjected to a uniform heat flux

$$\frac{\partial T^*}{\partial r^*} = Nh$$

where the wall heat-flux parameter Nh is defined by

$$Nh = \frac{q_w D}{k(T_s - T_j)} \tag{11}$$

The interface is at saturation temperature T_s and is assumed to be wave-free and shear-free

$$\frac{\partial v^*}{\partial x^*} = 0,\ T^* = 1 \quad \text{at} \quad x^* = \frac{H}{D}$$

The axial velocity at the interface is the condensation-induced velocity and is given, from Eq. (6), by

$$u^* = -u_c^* = -\frac{Ja\left(\frac{\partial T^*}{\partial x^*}\right)_s}{PrBRe_j} \quad \text{at} \quad x^* = \frac{H}{D} \tag{12}$$

It should be noted that although buoyancy force is neglected, the velocity and temperature fields are still coupled through the condensation-induced velocity u_c at the interface.

For the central jet, uniform velocity and temperature are assumed

$$u^* = 1, \quad v^* = 0, \quad \text{and} \quad T^* = 0$$

In order to maintain constant liquid level, the volume flow rate of the liquid withdrawn from the outer part of the tank bottom should be equal to the jet volume flow rate plus the condensation volume flow rate. With the assumption of uniform velocity and zero temperature gradient, the boundary conditions at the liquid-withdrawn plane are given by

$$u^* = -\frac{A_j}{A_{\text{out}}}\left[1 + \frac{Ja\overline{\left(\frac{\partial T^*}{\partial x^*}\right)_s}}{PrRe_j}\right]$$

and

$$v^* = 0, \quad \frac{\partial T^*}{\partial x^*} = 0$$

It is evident that there are seven relevant parameters governing the present problem:

$$Re_j,\ Pr, \text{ and } B \text{ (from the governing equations)} \tag{13}$$

$$\frac{H}{D},\ \frac{A_{\text{out}}}{A_j},\ Ja, \text{ and } Nh \text{ (from the boundary conditions)} \tag{14}$$

The average condensation heat-transfer coefficient, $\bar{h}_c$, and condensation Stanton number, $\overline{St}_c$, which describe the interfacial heat and mass transports, are defined as

$$\bar{h}_c = \frac{\bar{m}_c h_{fg}}{(T_s - T_j)} \tag{15}$$

$$\overline{St}_c = \frac{\bar{h}_c}{\rho u_j C_p} \tag{16}$$

By using Eq. (4) or (5), the average condensation Stanton number can be expressed as

$$\overline{St}_c = \frac{8\int_0^{0.5}\left(\frac{\partial T^*}{\partial x^*}\right)_s r^* dr^*}{Re_j BPr} \tag{17}$$

or

$$\overline{St}_c = \frac{Y}{Re_j BPr} \tag{18}$$

respectively, where

$$Y = \frac{\dfrac{(PrRe_j \bar{T}^*_{out})}{(D/d)} - 4Nh(H/D)}{1 + Ja(1 - \bar{T}^*_{out})}$$

and

$$\bar{T}^*_{out} = \frac{\bar{T}_{out} - T_j}{T_s - T_j}$$

From the above analysis, the condensation Stanton number can be expressed as

$$\overline{St}_c = f\left(Re_j, Pr, \frac{D}{d}, \frac{H}{D}, \frac{A_{out}}{A_j}, Ja, Nh\right) \tag{19}$$

The effect of Re_j and Pr on $\overline{St}_c$ has been studied in Ref. 7. This paper describes the effects of the other system parameters on the interface condensation process. It has been observed that, for $Re_j \leq 600$, the flow is still laminar for a similar tank system.[8] Thus, the present calculations are conducted for jet Reynolds number (Re_j) equal to 150, 200, and 300 which are in laminar flow range, and for Prandtl number (Pr) equal to 1.25 and 2.1 which represent typical values of liquid hydrogen and nitrogen, respectively. The ranges of the other parameters are $12.5 \leq D/d \leq 33.3$, $0.25 \leq H/D \leq 1.25$, $7.5 \leq A_{out}/A_j \leq 357$, $0 \leq Ja \leq 0.2$, and $0 \leq Nh \leq 4$.

Numerical Method of Solutions

The above elliptic partial differential equations are numerically solved by a finite-difference method. The finite-difference equations are derived by integrating the differential equations over an elementary control volume surrounding a grid node appropriate for each dependent variable.[9] A staggered grid system is used such that the scalar properties, p and T, are stored midway between the u and v velocity grid nodes. The bounded skew hybrid differencing (BSHD) is incorporated for the convective terms[9] and the integrated source terms are linearized. Pressures are obtained from a predictor-corrector procedure of the Pressure Implicit Split Operator (PISO) method[10] which yields the pressure change needed to acquire velocity changes to satisfy mass continuity. The governing finite-difference equations are solved iteratively by the ADI method with under relaxation until the solutions are converged.

Calculations are performed with a nonuniform grid distribution with concentration of the grid nodes in the centerline, near-wall, and near-interface regions where the gradients of flow properties are expected to be large. The nonuniform grid distribution in axial direction is generated by using an exponential function of Roberts' transformation[11] with the stretching parameter equal to 1.02. In the radial direction, the scheme used by Cebeci and Smith[12] with a constant ratio between two adjacent grid spacing is used. The 72 by 41 grid nodes, which have been shown in Ref. 7 to give reasonable grid-independent solutions, are used for all the calculations in the present study. Calculations are performed on a CRAY-XMP computer located at NASA Lewis Research Center. The convergent solutions are considered to be reached when the absolute value of Eqs. (17) and (18)/Eq. (17) is less than 0.005 and the maximum of absolute residual sums for each dependent variables is less than 10^{-6}.

Results and Analysis

Numerical solutions showed that the flowfield near the jet region is generally independent of the parameters Ja, Pr, Nh, and A_{out}/A_j at least for their ranges considered in this study. The linear relation between the potential core length to jet diameter ratio (x_p/d) and jet Reynolds number (Re_j) obtained in Ref. 7, $x_p/d = 0.0067\ Re_j$, is confirmed. The present calculations further show that the linear relation holds only when H/d is greater than some critical value. As shown in Fig. 2, larger Re_j and lower D/d tend to reduce the critical value of H/d. This is because the larger Re_j and d/D carry more jet momentum to resist the disturbance induced by the existence of free-surface.

The axial jet introduced from the bottom will turn radially outward from the center line as it approaches the interface. Numerical solutions indicate that the radial velocity at the interface v^*_s is essentially unaffected by Pr, Nh, and A_{out}/A_j. However, the v^*_s is a strong function of H/D and D/d and is slightly affected by Ja. Figure 3 gives the distributioin of radial interface velocity (v^*_s) as a function of Ja, H/D, and D/d. The v^*_s is increasing with Ja and decreasing with H/D and D/d. The peak value of v^*_s is located closer to the center line when

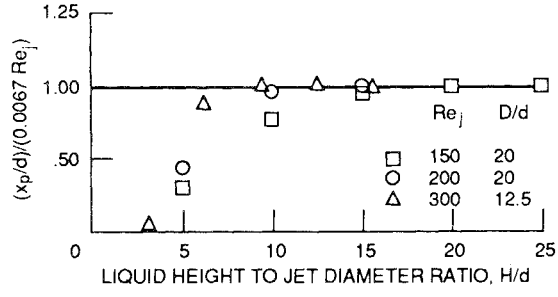

Fig. 2 Potential core length as a function of jet Reynolds number.

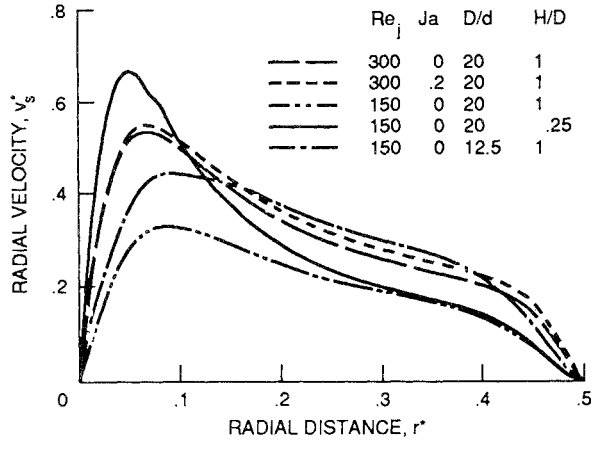

Fig. 3 Radial velocity distribution at the liquid-vapor interface for $Nh = 0$ and $Pr = 1.25$.

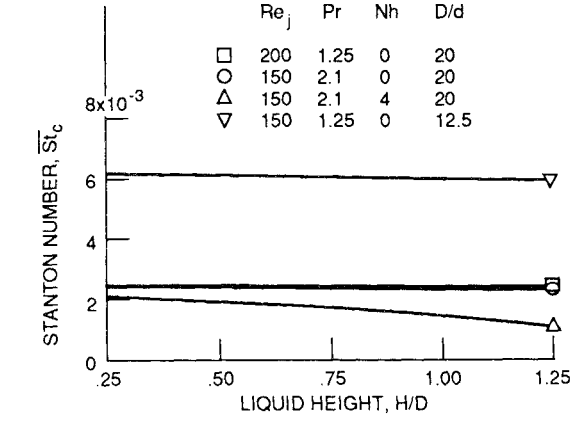

Fig. 4 Condensation Stanton number as a function of liquid level height for $Ja = 0$ and $A_{out}/A_j = 357$.

the parameters D/d and Re_j are larger, and Ja and H/D are smaller. However, it is generally located within the region of $r^* \leq 0.1$. Incorporated with the calculations of Ref. 7, the average value of v_s^* can be described by the following equation within ±3% of the exact numerical solutions:

$$\bar{v}_s^* = 0.2\, Re_j^{0.5} \left(\frac{H}{D}\right)^{-0.25} \left(\frac{D}{d}\right)^{-0.905} (1 + 0.226\, Ja) \quad (20)$$

for $H/d \geq 10$, $Ja \leq 0.2$, $150 \leq Re_j \leq 600$, $Nh \leq 4$, and $1.25 \leq Pr \leq 2.65$.

Calculations show that under adiabatic (or very low heat leak) conditions, $\overline{St}_c$ is essentially independent of the ratio A_{out}/A_j and the liquid-withdrawn location. However, additional calculations for high heat leak, $Nh = 4$, indicate that $\overline{St}_c$ is greater if the outflow location is closer to the tank wall. This is because the outflow located closer to the wall enhances the liquid circulation of the tank and convects more heat from the wall to gain a higher outflow temperature at the tank bottom. This information will be very useful in the design of a pumping system for the mixer.

The heat transfer due to condensation is carried away by the radial flow motion near the interface. Therefore, the interfacial heat transfer is expected to be greater for lower liquid fill level since the radial velocity near the interface will be greater. The variation of the average condensation Stanton number $\overline{St}_c$ with H/D is shown in Fig. 4. For an adiabatic wall, i.e., $Nh = 0$, $\overline{St}_c$ is a relatively weak function of H/D. However, with an increase in Nh, the average condensation rate decreases significantly as H/D increases. As for example, Fig. 4 shows that for $Nh = 4$ and $Re_j = 150$, the condensation rate at $H/D = 1.25$ is reduced by more than 60% compared to that at $H/D = 0.25$.

Figure 5 shows the the distribution of the interface temperature gradient for different values of H/D and D/d. The interface temperature gradient at the central part of the interface, $(\partial T^*/\partial x^*)_s$, increases as H/D decreases. However, $(\partial T^*/\partial x^*)_s$ decreases with a decrease in H/D at the outer part of the interface. In contrary to the effect of H/D, the interface temperature gradient at the central part decreases with a decrease in D/d, but increases appreciably at the outer part of the interface. The average value of the interface temperature gradient is greater for smaller D/d because the larger jet diameter introduces more jet flow rate to the tank. Also seen from Fig. 5, lower H/D and higher D/d result in the condensation being more confined in the central part of the interface. Thus, the normal-g (flat interface) solutions may be applied to the low-g condition if the liquid fill level is low and jet nozzle diameter is small enough. The effect of D/d on $\overline{St}_c$ is given in Fig. 6. For a given H/D, $\overline{St}_c/(d/D)^2$ approaches an asymptotic value. Thus, it can be stated that if D/d is large enough, $\overline{St}_c$ will be proportional to $(d/D)^2$. For $Ja \ll 1$ and $Nh \ll 1$, a correlation for predicting $\overline{St}_c$ (within ±5% bound) is given by

$$\overline{St}_c = 0.977 \left(\frac{H}{D}\right)^{-0.025} Pr^{-0.03} \left(\frac{D}{d}\right)^{-2} \quad (21)$$

for $0.25 \leq H/D \leq 1.25$, $0.85 \leq Pr \leq 2.65$, $150 \leq Re_j \leq 600$, and $D/d \geq 20$. It should be noted that although $\overline{St}_c$ is independent of jet Reynolds number Re_j for $Ja \ll 1$ and $Nh \ll 1$, this may not be true for larger values of Ja and Nh. From Eq. (21), it is evident that D/d is a more important parameter affecting the interface condensation than H/D and Pr. Since the exponents on H/D and Pr are so small, $\overline{St}_c = (d/D)^2$ may give a reasonably good prediction of interface condensation rate. In that case, $\overline{St}_c$ is determined by the system geometry and the interface condensation rate can be determined by the jet volume flow rate. From Eq. (18), the outflow temperature is essentially equal to the saturation temperature. However, from basic principles, the outflow temperature will inevitably fall below the saturation temperature at some point when Re_j is increased.

The jet subcooling is characterized by Jakob number (Ja). Figure 7 shows that $\overline{St}_c$ is linearly increasing with Ja. For an adiabatic wall ($Nh = 0$), the increase of $\overline{St}_c$ with respect to Ja is very small. The effect of Ja on $\overline{St}_c$ is enhanced at larger Nh. However, even for high-wall heat flux, $Nh = 4$, the difference in the value of $\overline{St}_c$ between $Ja = 0$ and 0.2 is still less than 4%. For most common cryogens such as liquid hydrogen, nitrogen, and oxygen, Ja is generally less than 0.2 for most practical applications. Thus, the effect of Ja can be neglected and the work of Ref. 7 in which $Ja = 0$ was assumed is also justified. It is noted that the explicit effect of Ja on $\overline{St}_c$ is directly through the condensation-induced velocity u_c^* at the interface. Thus, the negligible effect of Ja simply means that, whether u_c^* at the interface is included in the calculations or not, the effect is negligible. Numerical solutions show that the maximum value of u_c, which is usually located at or near the center line, is generally at least two orders of magnitude lower than the jet velocity. For instance, $(u_c/u_j)_{max}$ is about 0.0077 for $Ja = 0.2$, $Nh = 0$, $Re_j = 300$, $Pr = 1.25$, $H/D = 1.0$, and $D/d = 20$.

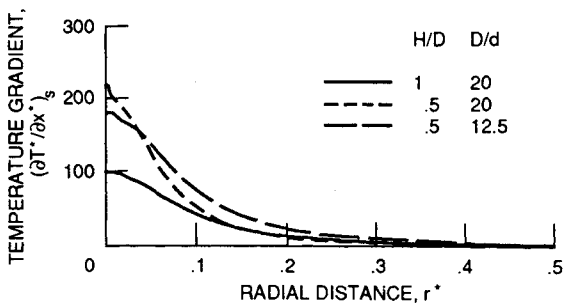

Fig. 5 Temperature gradient distribution at the interface for Re_j = 150, Pr = 1.25, Nh = 0, and Ja = 0.

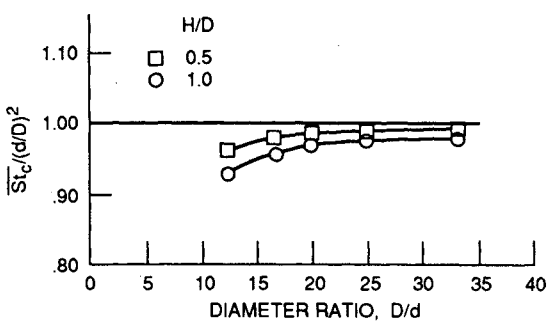

Fig. 6 Condensation Stanton number as a function of tank to jet diameter ratio for Re_j = 150, Pr = 1.25, Nh = 0, and Ja = 0.

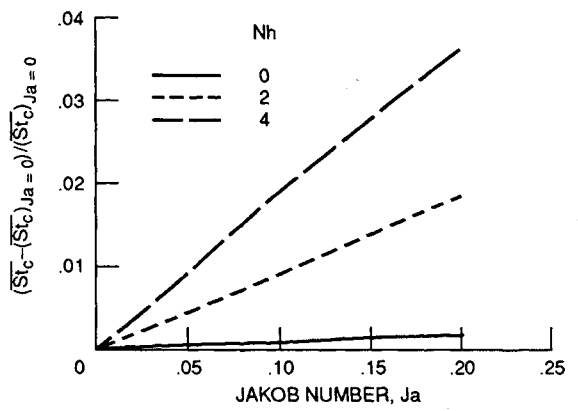

Fig. 7 The effects of Jakob number and wall heat-flux parameter on the average condensation Stanton number for D/d = 20, H/D = 1.0, Re_j = 300, and Pr = 1.25.

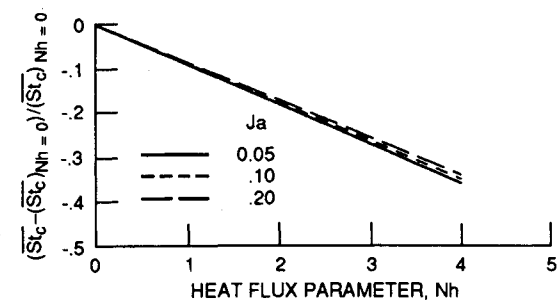

Fig. 8 The effects of wall heat-flux parameter and Jakob number on the average condensation Stanton number for $D/d = 20$, $H/D = 1.0$, $Re_j = 300$, and $Pr = 1.25$.

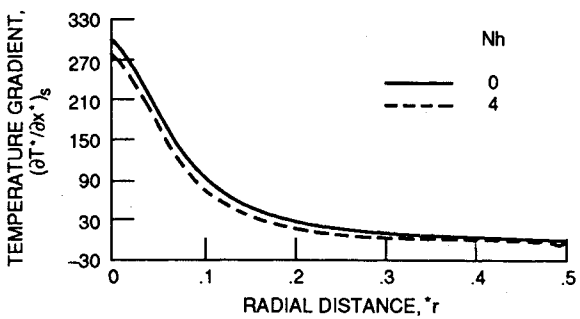

Fig. 9 Temperature gradient distribution at the interface for $H/D = 1.0$, $D/d = 20$, $A_{out}/A_j = 357$, $Re_j = 300$, $Pr = 1.25$, and $Ja = 0$.

Heat transfer through the tank walls generates thermal stratification and increases the jet temperature near the interface. For a fixed jet subcooling, an increase in the wall heat flux, i.e., an increase in Nh, results in the reduction of interface condensation. Figure 8 shows the linear relation between the average condensation Stanton number $\overline{St}_c$ and the heat leak parameter Nh. Figure 9 shows that the interface temperature gradient $(\partial T^*/\partial x^*)_s$ is lower everywhere for $Nh > 0$ (wall heat leak) than that for $Nh = 0$ (adiabatic wall). It is noted that if Nh is large enough, say $Nh = 4$, vaporization may occur at the interface near the tank wall. Thus, the value of $\overline{St}_c$ is significantly decreasing with increasing Nh and Eq. (21) is valid only for small Nh.

Conclusions

The effects of system parameters on the interface condensation rate in a laminar jet-induced mixing tank as shown in Fig. 1 have been numerically investigated. Based on the assumptions and parameter ranges considered, the following conclusions can be made:

1) The condensation rate is essentially independent of the outflow to jet area ratio, A_{out}/A_j, except for high wall heat flux.

2) The average condensation Stanton number, $\overline{St}_c$, linearly increases with Jakob number, Ja, and linearly decreases with the wall heat-flux parameter, Nh. The effect of Ja on $\overline{St}_c$ is enhanced when Nh is greater than zero.

3) The average condensation Stanton number, $\overline{St}_c$, is decreasing with increasing liquid height to tank diameter ratio, H/D, and tank to jet diameter ratio, D/d. The parameters D/d and Nh have stronger effects on $\overline{St}_c$ than the parameters H/D and Ja.

4) For $Ja \ll 1$ and $Nh \ll 1$, $\overline{St}_c$ will be essentially equal to $(d/D)^2$ if $D/d \geq 20$, $Re_j \leq 600$, and Pr and H/D are close to one. Thus, the interface condensation rate can be simply determined by the jet volume flow rate.

5) Lower values of H/D and d/D will yield condensation more confined at the central part of the interface. Thus, normal-g (flat interface) solution may be applied to the low-g (curved interface) condition if the liquid fill level is low and the jet nozzle diameter is relatively small.

References

[1]Aydelott, J. C., Carney, M. J., and Hochstein, J. I., "NASA Lewis Research Center Low-Gravity Fluid Management Technology Program," NASA TM-87145, 1985.

[2]Poth, L. J., and Van Hook, J. R., "Control of the Thermodynamic State of Space-Stored Cryogens by Jet Mixing," *Journal of Spacecraft and Rockets*, Vol. 9, No. 5, 1972.

[3]Thomas, R. M., "Condensation of Steam on Water in Turbulent Motion," *International Journal of Multiphase Flow*, Vol. 5, No. 1, 1979, pp. 1–15.

[4]Dominick, S. M., "Mixing Induced Condensation Inside Propellant Tanks," AIAA Paper 84-0514, 1984.

[5]Sonin, A. A., Shimko, M. A., and Chun, J. H., "Vapor Condensation onto a Turbulent Liquid-I. Steady State Condensation Rate as a Function of Liquid-Side Turbulence," *International Journal of Heat Mass Transfer*, Vol. 29, No. 9, 1986, pp. 1319–1332.

[6]Hasan, M. M., and Lin, C. S., "Axisymmetric Confined Turbulent Jet Directed Towards the Liquid Surface From Below," AIAA Paper 89-0172; also NASA TM 101409, 1989.

[7]Lin, C. S., "Numerical Studies of the Effects of Jet-Induced Mixing on Liquid-Vapor Interface Condensation," AIAA Paper 89-1744, 1989.

[8]Sonin, A. A., "Basic Transport Phenomena for Application to Cryogenic Fluid Management in Space." Progress Rept., NAG3-731, NASA LeRC, Jan. 1990.

[9]Syed, S. A., Chiappetta, L. M., and Gosman, A. D., "Error Reduction Program," NASA CR-174776, 1985.

[10]Issa, R. I., "Solution of Implicitly Discretised Fluid Flow Equations by Operator-Splitting," *Journal of Computational Physics*, Vol. 62, No. 1, 1986.

[11]Roberts, G. O., "Computational Meshes for Boundary Layer Problems," *Proceedings of the Second International Conference Numerical Methods Fluid Dynamics, Lecture Notes in Physics*, Vol. 8, Springer-Verlag, New York, 1971, pp. 171–177.

[12]Cebeci, T., and Smith, A. M. O., *Analysis of Turbulent Boundary Layers*, Academic Press, New York, 1974.